A triaxiality-dependent fracture model for hot-rolled sections made of S355 steel

Kastiza, Pelagia; Skalomenos, Konstantinos; Theofanous, Marios

DOI:
10.1002/cepa.2693

Document Version
Publisher's PDF, also known as Version of record

Citation for published version (Harvard):
Kastiza, P, Skalomenos, K & Theofanous, M 2023, 'A triaxiality-dependent fracture model for hot-rolled sections made of S355 steel', *ce/papers*, vol. 6, no. 3-4, pp. 2570-2575. https://doi.org/10.1002/cepa.2693

ce/papers Proceedings in civil engineering

Ernst & Sohn A Wiley Brand

ORIGINAL ARTICLE

eurosteel AMSTERDAM 2023

Ernst & Sohn A Wiley Brand

A triaxiality-dependent fracture model for hot-rolled sections made of S355 steel

Pelagia Kastiza[1] | Konstantinos Skalomenos[1] | Marios Theofanous[1]

Correspondence

Dr. Konstantinos Skalomenos
Department of Civil Engineering
School of Engineering
University of Birmingham
Birmingham
B15 2TT Edgbaston
United Kingdom
Email: k.skalomenos@bham.ac.uk

[1] School of Engineering, University of Birmingham, Birmingham, United Kingdom

Abstract

Fracture at net areas of steel sections often leads to premature failures of steel members, especially in the region of joints (bolted connections). This study develops a fracture model for hot rolled S355 steel for enabling a better understanding of the ultimate behaviour of steel sections through numerical simulations using the general-purpose finite element software ABAQUS. Monotonic tensile tests are conducted on traditional dog-bone plate specimens with a uniform cross-section and notched plate specimens extracted from hot-rolled I-beams. Two material thicknesses and three notch radii per thickness are considered thus obtaining equivalent plastic strains at fracture over a wide range of stress triaxialities. The experimental fracture displacement is used as a threshold for the determination of the average stress triaxiality – equivalent strain history at the critical location (fracture initiation) of each plate model. Using regression analysis, an exponential approximation of the fracture locus is proposed to correlate the average stress triaxiality for a given equivalent plastic strain at fracture. The proposed model is then used to predict fracture initiation of unnotched tensile coupons and steel plates with a bolt hole in their centre extracted from the same steel sections. The test results are in good agreement with the numerical predictions thus demonstrating the efficiency of the proposed method.

Keywords Fracture model, average triaxiality, equivalent plastic strain, necking behaviour, FEM, GMNIFA

1 Introduction

With the advancement of numerical modelling, geometrically and materially nonlinear structural analysis incorporating initial geometric imperfections (GMNIA) has become a mature technology in structural engineering thus allowing failure modes triggered by buckling to be accurately simulated. However, GMNIA fails to accurately simulate failures triggered by material fracture, which is often the case in steel connections. To this end the development of GMNIFA (geometrically material nonlinear imperfection and fracture analysis) is currently underway by incorporating explicit fracture models in the definition of the material response.

Steel structures are widely used in construction due to their numerous advantages. Some of their notable characteristics include their high ultimate strength and ductility, their cost-effectiveness (prefabrication can be done off-site reducing to the minimum the construction time and fabrication cost), and their environmental sustainability. Steel is almost 100% recyclable.

However, steel structures are vulnerable due to corrosion effects, welding defects or inadequate design of net sections, leading potentially to a significant reduction of their ductility and premature fracture at high-stress locations, such as in the vicinity of bolt holes in connections. Connection failure is the most common premature failure in steel structures, leading to catastrophic incidents including collapse of structures [1].

Over the last decades a significant progress has been made in finite element methods (FEM) for the nonlinear analysis of the structural response. The growing demand for high-performance steel structures requires no premature fracture on stress concentration areas, thus allowing the structure to develop its full potentials in terms of ultimate strength and ductility. Developing a numerical fracture model that can accurately predict the behaviour of areas of high stress concentration is essential to adequately predict global ductility and optimize the design of the structural system.

Numerical fracture models, based on previous research [2]

https://doi.org/10.1002/cepa.2693 wileyonlinelibrary.com/journal/cepa

can fall into two main categories: (1) the damage mechanics-based models that calculate damage throughout loading history, and (2) the critical strain or state-based models which provide fracture criteria independent of the continuum parameter's history, but based on constant values. The damage mechanics-based models can be further classified as coupled and uncoupled models, in terms of including the material softening response as a part of the fracture criterion or not [2,3].

Some well-established uncoupled models have been developed and validated for different structural steel grades. The Void Growth Model, introduced by Panontin and Sheppard (1995) and Kanvinde and Deierlein (2006), has been calibrated for the ASTM A992 structural steel and steels similar to Grade 50 steel, by using the theoretical material parameter defined by Rice and Tracey (1969) [2,3]. Later, Khiran and Khandelwal (2013) investigated the fracture mechanism of ASTM A992 structural steel by calibrating the VGM to obtain the material specific constant based on the minimum coefficient of variation, instead of using the theoretical material parameter [4]. Finally, the model developed by Jia and Kuwamura (2013) has been calibrated on unnotched specimens and validated in mild structural steels STKR400 [5] and duplex stainless steel [6].

In the current study an uncoupled damage mechanics-based fracture model has been developed that can accurately predict fracture initiation for grade S355. It is notable that there is no such fracture model available in literature for S355 steel. The developed model uses a plasticity model that minimizes the inaccuracy in material flow stress prediction and follows the Bao and Wierzbicki's concept [7] of average stress triaxiality. Finally, the proposed model can be easily implemented in FEM and through additional validation material tests is proved to be accurate enough in predicting fracture initiation and location, as well as the triggered triaxiality mechanism.

2. Damage modelling

In Abaqus ductile fracture is simulated through four distinct phases. Figure 1 shows the typical stress strain curve of a ductile material including the following phases: the definition of the undamaged material response (a-b-c-d'), the establishment of a damage initiation criterion at the onset of the strength degradation (c) where the overall damage variable is equal to zero (D=0), the determination of a damage evolution law (c-d), and the element deletion by default upon reaching maximum degradation (D=1) at point d [8]. However, in the currently developed model, point c does not represent the damage onset, but the initiation of the necking where the plastic response becomes nonuniform and strain localisation occurs. Note that necking behaviour is simulated by using a proper size of mesh elements as it is discussed in a later section. The fracture initiation criterion instead, is defined at the point **e** of the solid curve, that corresponds to the experimental fracture displacement. Beyond this point, the material loses completely its load carrying capacity and element deletion occurs; this is achieved by defining a negligible fracture energy (damage evolution) accompanied by the automatic element deletion.

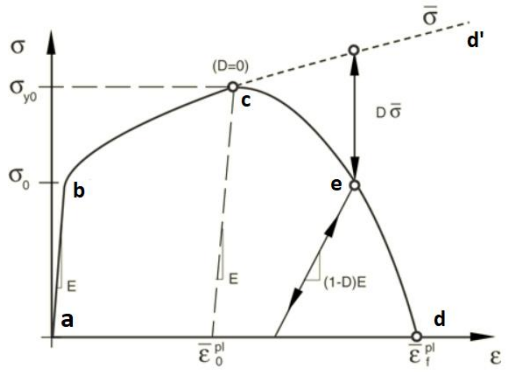

Figure 1 The stress-strain curve of a typical ductile material [8] based on the distinct faces that Abaqus outlines the failure mechanism. The solid line represents the damaged material and the dashed, the undamaged.

3. Methodology steps

The proposed fracture model describes the critical conditions for fracture initiation accounting for the stress triaxiality and plastic deformation history until the failure point. The ductile fracture mechanism that underpins the model states that fracture initiation happens under uniaxial tension due to the growth of microvoids and their rapid coalescence. The fracture model development methodology utilises a combination of experimental and iterative numerical techniques, which consist of the following steps:

Step 1: Axial tensile tests on notched plates and unnotched specimens are conducted. The unnotched tensile tests are caried out to study the behaviour and mechanical properties of S355 steel, and the notched specimens are tested to create a wide range of stress triaxialities and corresponding strains at fracture to allow the triaxiality dependence of the material to be quantified.

Step 2: Refined FEM simulations are conducted for the unnotched test specimens to verify the selection of the appropriate material model that accurately predicts the experimental stress-strain curve calibrating the material stress-strain curve to accurately approximate the material behaviour post necking, using the Weighted Average Method (WAM) [9].

Step 3: FE models of the notched plate specimens are then generated and subjected to uniaxial tension up to the fracture displacement obtained from tests.

Step 4: The stress triaxiality and equivalent plastic strain histories for the critical element (i.e. point of ductile fracture initiation, corresponding to the maximum triaxiality-equivalent plastic strain) are obtained from the start of the loading until the experimental fracture displacement. The average stress triaxiality, based on Bao and Wierzbicki concept [7], is calculated at the experimental failure displacement as the integral of the triaxiality-equivalent plastic strain curve divided by the equivalent plastic strain at fracture initiation.

Step 5: The average triaxiality and equivalent plastic strain values at fracture are plotted together for all the notched specimens tested, thus allowing a relationship between the two to be obtained. The exponential model was chosen due to its ability to minimize relative error among all data points analysed. This decision was supported by

prior research indicating an exponential relationship between these parameters [3-7].

3.1 Experimental procedure

Based on the presented methodology, uniaxial tensile coupon tests on notched plates and unnotched specimens should be carried out. Four flat coupons were tested for each category to ensure repeatability of the results, while the average experimental stress strain curves are used for the numerical validation of the tests. Universal beams made of hot-rolled steel S355J0 grade were used to extract the coupons. All the specimens were cut in parallel with the rolling direction of the hot-rolled section. Unnotched dog bone type specimens of two thicknesses were considered: 4.8mm and 7.9mm. All specimens had a total length of 300mm and width of 40mm, while their ungripped length was equal to 150mm. They all had a reduced area with width of 30 mm over a deformable length of 80mm. All the tested specimens were clamped in the jaws of the testing machine. Figure 2 shows the dimensions details of the unnotched specimens, while Figure 3 shows the arrangement of the coupons in the testing machine.

Uniaxial tension testing was performed on the specimens in accordance with ASTM E8 (ASTM 2009) guidelines, by using an Avery Universal testing frame system. The mechanical testing was conducted with strain measurements obtained through contact extensometers. The specimens were loaded at a rate of 0.02 mm/s and strains were measured over a 50 mm gauge length. The same tensile testing conditions have been applied to both unnotched and notched specimens.

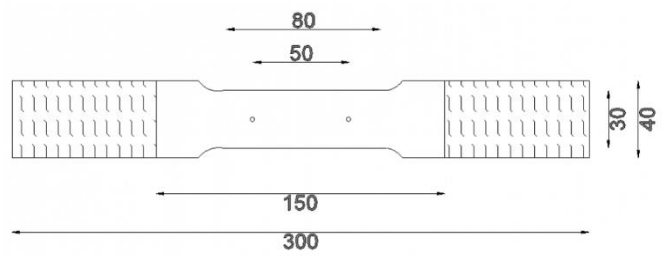

Figure 2 Illustration of the unnotched specimens including the gripped edges. The dimensions are given in mm.

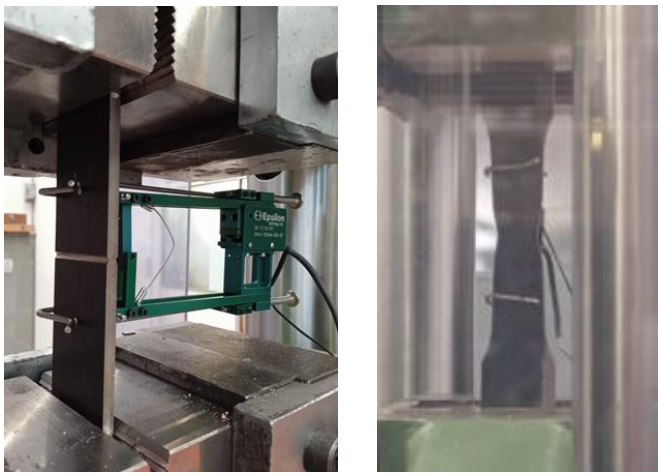

Figure 3 A tested notched specimen with the extensometer attached at the ends of the gauge length (left), observation of the necking in the reduced area of an unnotched specimen during testing (right).

From hot rolling procedure a variety of thicknesses can be generated. Triaxiality is a concern under plane strain conditions, where deformation occurs primarily in two dimensions and the thickness is significant enough to influence the stress state. In this study flat grooved plate plane strain specimens of two different thicknesses (i.e. 4.8mm and 7.9mm) are considered to examine their influence on the triaxiality mechanism. To expand the range of triaxiality, notched tensile tests induce an elevated triaxial state in the notched region. This, in turn, leads to a broader spectrum of stress triaxialities, impacting both fracture initiation and overall ductility. Different notches are machined on the plates to determine variations of the triaxial stresses and strains within the specimen in order to establish the relationship between the fracture strain and stress triaxiality with the maximum possible number of data sets. The three different notch sizes that were machined on flat plates (R1.6, R3.5, R12) and the two different thicknesses of the original plates resulted in a wide range of stress triaxialities and fracture strains. The machined radii satisfied a wide range of triaxialities in the tensile area corresponding to high triaxialities (0.9-1.1) for radius 1.6mm, medium triaxialities (0.8-0.9) for radius of 3.5mm and low triaxialities (0.5-0.7) for radius equal to 12mm. It has been observed that the smaller the notch radius the higher the triaxiality. For uniaxial stress state, the stress triaxiality is equal to 1/3 [7]. The fracture model is developed for a triaxiality range from 0.4 to 1.1; values that are extracted from the combination of two thicknesses (4.8, 7.9mm) with three different notch radii. Higher range of thickness may affect the triaxiality but its wider range will remain the same.

The initial stress triaxiality for a flat notched plate is calculated based on the geometry of the tested specimens and is represented by the dimensionless stress triaxiality ratio η, which is defined as

$$\eta = \frac{\sigma_m}{\sigma_{eq}} = \frac{\sqrt{3}}{3}\left[1 + 2\,ln\left(1 + \frac{t}{4R}\right)\right] \quad (1)$$

Where σ_m is the hydrostatic stress, and σ_{eq} is the equivalent von Mises stress, R is the radius of each circumferential notch and t is the ligament thickness of each flat plate [7].

The equivalent strain to fracture in the necking cross section of a flat notched plate can be determined using the logarithmic measure of the true strain. The average strain in fracture based on [7] is defined as

$$\bar{\varepsilon}_f = \frac{2}{\sqrt{3}}\,ln\left(\frac{t_0}{t_f}\right) \quad (2)$$

Where t_0 is the initial ligament thickness of the specimen and t_f is the ligament thickness of the specimen at fracture.

In the current study the concept of the average triaxiality is adopted as shown in Eq. (3). This concept has been suggested in [7] and, accounts for the fact that the stress triaxiality is not a constant value in the plastic deformation process, but it changes along the loading history and is affected by the change in geometry of the tested specimen. For that purpose there is a necessity for numerical simulation of the notched tests where the histories of stress triaxiality and the equivalent plastic strain are obtained (see Step 4) [7].

$$\eta_{ave} = \frac{1}{\bar{\varepsilon}_f}\int_0^{\bar{\varepsilon}_f} \eta(\bar{\varepsilon})d\bar{\varepsilon} \quad (3)$$

3.2 Material modelling

In the material model of ABAQUS, elastic-plastic material models with a combined isotropic hardening limited to half cycle test data of a unidirectional tension test was adopted for the S355 steel. To accurately determine the behaviour of the material under deformation, it is essential to obtain true stress and true strain, by assuming that the stress and strain are uniform across the cross-section of the coupon, as long as it remains in a uniaxial state (i.e. prior to necking) [9]. The true strain is related with the engineering strain (i.e. as obtained from the test) by

$$\varepsilon = \ln(1 + e) \tag{4}$$

The true stress is related with the engineering stress (i.e. as obtained from the test) by

$$\sigma = s \times (1 + e) \tag{5}$$

Where, s is defined as the engineering stress and e, the corresponding engineering strain. The above assumption is valid until the initiation of necking. After necking, there is strain localization in the necked region, the area reduces, and the stress state becomes triaxial. To obtain true stress and true strain after necking, the weighted average method (WAM) is used by the assumption that ε_u is the true strain at which the engineering necking starts and σ_u the corresponding true stress [9]. The WAM, proposed by Ling in 1996, assumes an empirical lower bound and a linear upper bound for the true stress-true strain relationship after necking. The empirical lower bound is a power law curve that can be extrapolated by fitting the true stress-true strain curve before necking. This method provides an accurate way to estimate the true stress and true strain after necking initiation and applies to both flat and round samples, defined by the following formula.

$$\sigma = \sigma_u \left[w(1 + \varepsilon - \varepsilon_u) + (1 - w)\left(\frac{\varepsilon^{\varepsilon_u}}{\varepsilon_u^{\varepsilon_u}}\right)\right] \tag{6}$$

The experimental tensile load-extension curve after the initiation of the necking is considered as target and the true stress-true strain relation is searched for, iteratively by finite element analysis (FEM) until the target is reached within a certain tolerance by the choice of the suitable weighted factor, w. Finally, it is observed that the weight constant decreases with increasing yield-to-tensile ratio (Y/T), while higher Y/T ratio correlates with steeper post-necking gradient.

3.3 Numerical procedure and fracture model development

Both the plasticity and fracture model were numerically validated using tensile unnotched and notched tests, respectively.

For the numerical modelling a non-linear FEM code is applied. The ABAQUS/Standard solver is used for the material model validation and for the fracture model generation, while the ABAQUS/Explicit solver, that handles high nonlinear problem such as fracture, is used for the numerical/experimental validation of the fracture model followed by element deletion when the fracture initiates. Only one eighth of each specimen is modelled to reduce the computational time, and symmetric boundary conditions are applied on its three sides with the top end subjected to displacement loading. Boundary conditions and displacement loading were directly applied to the reference points at the bottom and top ends of the models. Figure 4 illustrates the one eighth models developed for both the notched and unnotched specimens, including their mesh refined zones. Eight-node linear solid elements with reduced integration, C3D8R were adopted and mesh refinement has been applied into the fracture zone. A mesh size of 0.3 mm was deemed as suitable to capture necking on the unnotched specimens and to account for the strain gradient's sharp ascent in the notch area where the initiation of failure is expected to occur.

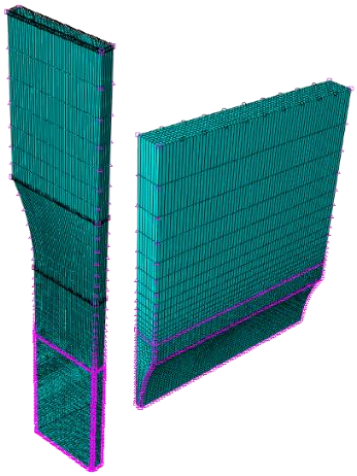

Figure 4 One eighth models corresponding to the unnotched specimens (on the left) and to the notched ones- scaled up (on the right) with obvious the mesh refinement (0.3mm) on the fracture area.

The unnotched tested specimens are numerically simulated first to confirm that the engineering stress-strain curves obtained from FEM agree well with the experimental ones by the application of the WAM and the choice of the suitable weighted factor for the optimum prediction of the material softening branch.

The modelling of the notched tests without failure criterion is required for the purpose of the calibration aim instead of validation. Each notched sample is loaded under its experimental failure displacement and the triaxiality and cumulative plastic strain histories are obtained for the critical element where ductile fracture is expected to initiate. Crack initiates at the centre of the cross section of the smoothly notched coupons and propagates quickly to the whole section. At the centre, the constraint is higher and both the triaxiality and strain acquire their maximum values over the loading history [2-4].

For the calibration of the ductile fracture model the average triaxiality and the equivalent plastic strain at failure needs to be estimated for every single notched sample model for the displacement that has led the equivalent experiment at failure. Then the total number of the numerical test sets of the average stress triaxiality and equivalent plastic strain at failure are plotted, and the exponential-type relationship that gives the minimum relative error is extracted and used as the final fracture criterion (7).

Where η is the triaxiality. Figure 5 illustrates the developed fracture model along with the stress triaxiality evolutions of both the notched and unnotched samples.

$$\varepsilon_f = 1.95 \times e^{-1.465\,\eta} \quad (7)$$

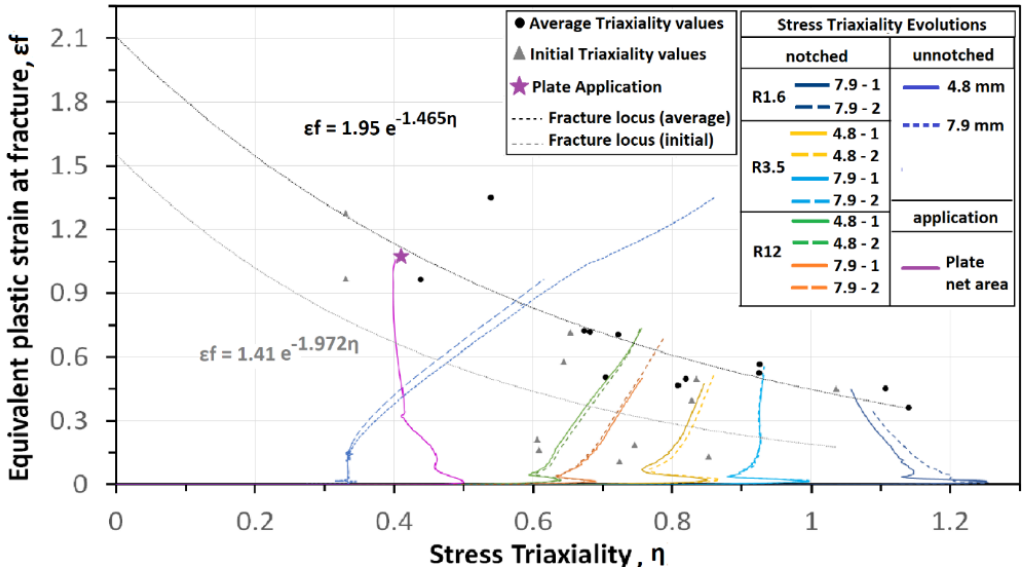

Figure 5 Fracture locus of steel S355 from numerical simulations using average stress triaxiality, black dots. The evolution of stress triaxiality for the flat grooved specimens, different dashed curves, and the initial triaxiality fracture locus is plotted, grey triangles.

4. Results

4.1 Validation of the material model

It is observed that for the unnotched specimens, the numerical stress-strain curves agree well with the experimental ones, for a weight constant, w, equal to 0.3 for thickness 4.8mm and equal to 0.35 for thickness 7.9mm. It is concluded that the weighted-average method predicts the true stress-strain relation after the onset of necking with high accuracy. Consequently, the true stress-strain relationship is established and can be used for both the notched and unnotched specimens. The coupon test results are presented in Table 1.

Table 1 Unnotched coupon test results

SPEC ID	Grade	Section Type	Ultimate Strength UTS (MPa)	Ultimate strain εu (%)	Yield Stress YS (MPa)	Yield Strain εy (%)	YS/UTS	WAM constant, W
IPE_4.8mm	S355	I-BEAM	508.89	16.3	403.08	0.22	0.79	0.30
IPE_7.9mm			507.86	17.9	371.83	0.22	0.73	0.35

4.2.1 Unnotched dog-bone coupons

The calibrated fracture strain-triaxiality dependent fracture model was implemented in the ABAQUS/Explicit simulations for the unnotched specimens. When the equivalent plastic strain of an element reaches the fracture strain indicated by the fracture model, the element deletion is automatically activated and failure initiates. Figure 6 shows the comparison between the experimental and the numerical curve (FEM) with the fracture criterion being applied for both the thicknesses of the unnotched specimens, 4.8mm and 7.9mm respectively. It is observed that the developed model predicts the failure with high accuracy in terms of initial stiffness, strength, and fracture displacement, for both unnotched specimens.

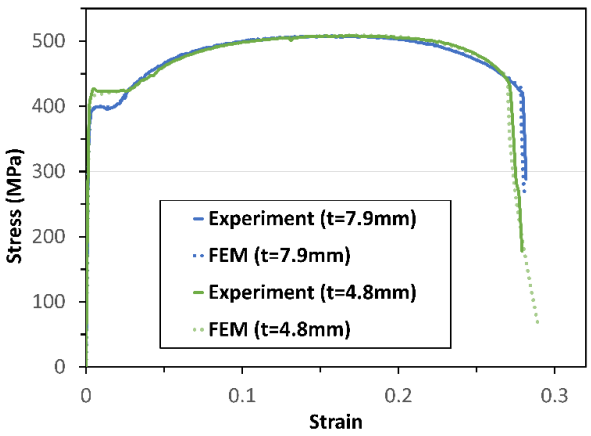

Figure 6 Comparison of the experimental and the numerical curve with fracture criterion for the unnotched specimens of 4.8 and 7.9mm.

4.2.2 Plates with net section

A plate was extracted from the centre of the web of the I-beam section having a total length of 400mm and a thickness of 4.8mm. A hole was cut at its centre with diameter equal to 4.54mm. The plate was subjected to tensile loads until fracture. During the experiment, the force was monitored by the testing machine, while a digital image correlation (DIC) system was used to measure the displacement and monitor the strain distribution. A finite element model with mesh refinement around the hole (elements size=0.3mm) was developed for validation purposes and DIC data were only used to capture crack initiation in the surface component and monitor the progress of crack growth during the validation test [10].
The experimental length, outside the jaws, was equal to

260mm, however, the comparison between the experiment and FEM was conducted for a plate length equal to 170mm (placing the hole at the centre). This is due to the limitation in length that the DIC system was calibrated for. Figure 7 compares the experimental and FEM results. It can be seen that strain concentration in FEM follows well that of DIC. Fracture initiated at the lateral edges of the hole and quickly expanded towards the plate edges. Figure 8 compares the force – displacement curves as obtained from the FEM and the test. A good agreement is observed between the analysis and the test as the fracture model fits the high strain concentration areas predicting the fracture point with accuracy. It is noted that the value of the average stress triaxiality at the critical element of the fracture initiation was found to be 0.42 and the cumulative plastic strain equal to 1.06.

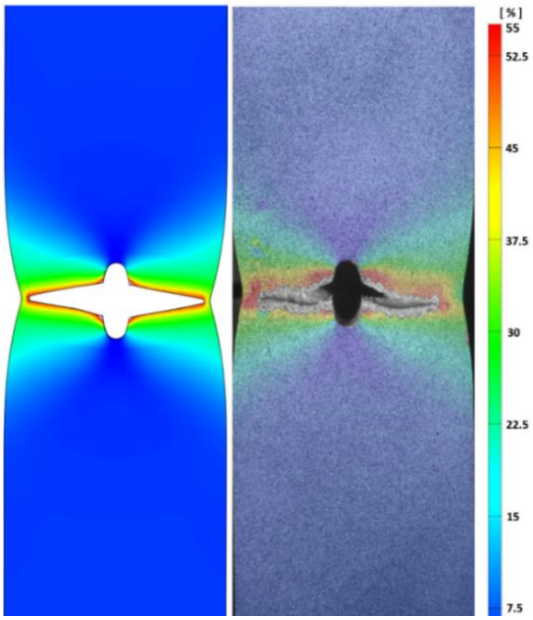

Figure 7 Comparison between the FEM and DIC Strain distribution on the plate indicating strain concentration over 50% at the lateral edges of the hole during fracture evolution.

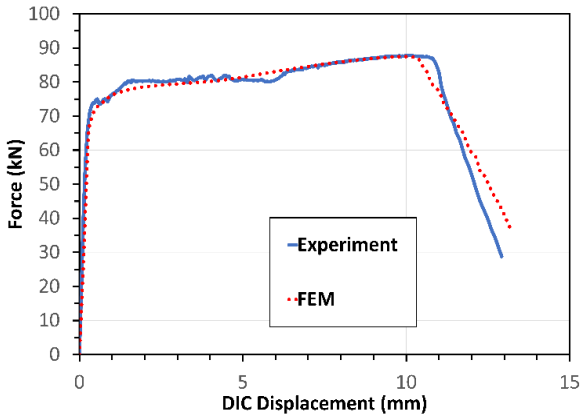

Figure 8 Comparison of the F-D experimental and numerical curve including the fracture criterion for the 4.8mm plate with net area at centre.

5. Conclusions

This paper develops a fracture model to predict the ductile failure of hot-rolled S355 steel sections using refined finite element methods. The main conclusions are as follows:

- The combined isotropic hardening model and the Weighted Average method predicted accurately the material response.
- It appears to be a correlation between the yield-to-tensile (Y/T) strength ratio and the WAM gradient of the necking branch (the higher the ratio, the steeper the necking). Additionally, the weight constant used in the WA method to predict the material softening it seems to decrease as the Y/T increases.
- The fracture model accurately predicted the rupture displacements of the experiments. Even for the application on the net area of the plate, it fitted the high concentration areas for average triaxiality equal to 0.42 and fracture strain of 1.06 (fig.5).
- Although they are approximate, uncoupled models can be easily implemented in FEM and provide a high degree of accuracy compared to the computationally expensive and mesh dependent coupled fracture models.

References

[1] Wardhana K.; Fabian C. H.; (2003) *Study of recent building failures in the United States, Journal of Performance of Constructed Facilities*, 17(3):151-158

[2] Kanvinde A.M.; (2017) *Predicting Fracture in Civil Engineering Steel Structures: State of the Art, Journal of Structural engineering*, 143(3): 03116001

[3] Kanvinde A.M.; Deierlein G.G.; (2006) *The Void Growth Model and the Stress Modified Critical Strain Model to Predict Ductile Fracture in Structural Steels, Journal of Structural engineering,* 132(12):1907-1918

[4] Kiran R.; Khandelwal K.; (2014) *Experimental Studies and Models for Ductile Fracture in ASTM A992 Steels at High Triaxiality*, *Journal of Structural engineering*, 140(2):04013044

[5] Jia L.; Kuwamura H.; (2014) *Ductile fracture simulation of structural steel under monotonic tension, Journal of Structural engineering*, 140(5): 04013115

[6] Ghorbanzadeh B.; Bregolia G.; Vasdravellis G.; Karavasilis T.L.; (2019) *Pilot experimental and numerical studies on a novel retrofit scheme for steel joints against progressive collapse*, *Journal of Engineering Structures*, 200: 109667

[7] Bai Y.; Wierzbicki T.; Teng X.; (2009) *On the Application of Stress Triaxiality Formula for Plane Strain Fracture Testing*, *Journal of Engineering Materials and Technology*, 131(2): 021002

[8] ABAQUS; (2020), *Analysis User's Manual, Dassault Systemes,* Version 6.14

[9] Ling Y.; (1996) *Uniaxial True Stress-Strain after Necking, AMP Journal of Technology*, 5

[10] Ghafoori E.; Motavalli M.*;* (2011) *Analytical calculation of stress intensity factor of cracked steel I-beams with experimental analysis and 3D digital image correlation measurements*, Journal of engineering fracture mechanics, 78: 3226–3